X Congreso Regional Latinoamericano IRPA de Protección y Seguridad Radiológica
"Radioprotección: Nuevos Desafíos para un Mundo en Evolución"
Buenos Aires, 12 al 17 de abril, 2015
SOCIEDAD ARGENTINA DE RADIOPROTECCIÓN

GENE EXPRESSION PROFILE ASSOCIATED WITH RADIORESISTANCE AND MALIGNANCY IN MELANOMA

Ibañez, I.L. [1,2,*], García, F.M.[3], Bracalente, C.[2], Zuccato, C.F.[4], Notcovich, C.[1], Molinari, B.[1,2], Durán, H.[1,2,3]

[1] Comisión Nacional de Energía Atómica, Argentina
[2] Consejo Nacional de Investigaciones Científicas y Técnicas (CONICET), Argentina
[3] Universidad Nacional de San Martín, Argentina
[4] Universidad Argentina de la Empresa, Argentina

ABSTRACT

The incidence of melanoma has substantially increased over the last decades. Melanomas respond poorly to treatments and no effective therapy exists to inhibit its metastatic spread. The aim of this study was to evaluate the association between radioresistance of melanoma cells and malignancy. A melanoma model developed in our laboratory from A375 human amelanotic melanoma cells was used. It consists in two catalase-overexpressing cell lines with the same genetic background, but with different phenotypes: A375-A7, melanotic and non-invasive and A375-G10, amelanotic and metastatic; and A375-PCDNA3 (transfected with empty plasmid) as control.
Radiosensitivity was determined by clonogenic assay after irradiating these cells with a Cs^{137} gamma source. Survival curves were fitted to the linear-quadratic model and surviving fraction at 2 Gy (SF2) was calculated. Results showed that A375-G10 cells were significantly more radioresistant than both A375-A7 and control cells, demonstrated by SF2 and α parameter of survival curves: SF2=0.32±0.03, 0.43±0.16 and 0.89±0.05 and α=0.45±0.05, 0.20±0.05 and 0 for A375-PCDNA3, A375-A7 and A375-G10 respectively.
Bioinformatic analysis of whole genome expression microarrays data (Affymetrix) from these cells was performed. A priori defined gene sets associated with cell cycle, apoptosis and MAPK signaling pathway were collected from KEGG (Kyoto Encyclopedia of Genes and Genomes) to evaluate significant differences in gene set expression between cells by GSEA (Gene Set Enrichment Analysis). A375-G10 showed significant decrease in the expression of genes related to DNA damage response (ATM, TP53BP1 and MRE11A) compared to A375-A7 and controls. Moreover, A375-G10 exhibited down-regulated gene sets that are involved in DNA repair, checkpoint and negative regulation of cell cycle and apoptosis.
In conclusion, A375-G10 gene expression profile could be involved in radioresistance mechanisms of these cells. Thus, this expression profile suggests that A375-G10 could escape from DNA damage-induced apoptosis with the consequent progression in the cell cycle resulting in genomic instability and increase of malignancy.

1. INTRODUCTION

The global incidence of melanoma reveals approximately 200,000 new cases and 65,000 melanoma-associated deaths each year [1, 2]. Although cutaneous melanoma accounts for only 4 % of all skin cancers; it causes the greatest number of skin cancer-related deaths worldwide [3]. Although surgery is an effective treatment when the disease is identified early melanomas are aggressive tumors with advanced disease characterized by widespread metastatic lesions. Moreover, melanoma has traditionally been resistant to most forms of treatment [4]. In order to better understand the multiple events involved in tumor progression

* E-mail: irenuliz@yahoo.com

and resistance to conventional treatments in advanced stages of the disease, the study of the molecular machinery associated with the genotype and phenotype of invasive malignant melanoma becomes relevant.

The intrinsic radiosensitivity of tumor cells is an important factor for determining radiotherapy efficacy [5]. During tumor development, changes in apoptosis induction, cell cycle control and oncogenes activation [5, 6] may modulate the radiosensitivity of tumor cells. The capacity to carry out repair when DNA is damaged by ionizing radiation is a critical factor in determining cellular radiosensitivity [5]. Ionizing radiation produces a broad spectrum of molecular lesions to DNA, including single strand breaks (SSBs), double strand breaks (DSBs), and a great variety of base damages. DSBs are the most toxic form of DNA damage, because a single unrepaired DSB can lead to abnormal mitosis with losses of large fragments of DNA [7]. It has been shown that the few DSBs that are produced by ionizing radiation correlate closely to the amount of induced cell death. DSBs are mainly repaired through homologous recombination repair (HRR) and nonhomologous end joining (NHEJ). Both mechanisms are initiated by the activation of ataxia telangiectasia mutated (ATM) kinase. ATM and its downstream kinase CHK2 phosphorylate several targets that regulate DNA repair, cell cycle and apoptosis, including H2AX, MDM2 and p53/p21 [8]. During the S and G2 phase of the cell cycle, DNA DSB repair occurs via homologous recombination. HRR restores DNA DSBs using the undamaged homologous chromosome as a template. This mechanism involves several proteins, including Rad51, -52 and -54, as well as BRCA1 and -2 and XRCC2 and -3 [9]. An alternative mechanism, NHEJ, operates throughout the cell cycle. It effectively links up the ends of broken DNA in a chromosome without a template. This is the major route for the repair of radiation-induced DSB. XRCC4 and -5, DNA-PKcs and LIG4 are downstream effectors in NHEJ [10]. Deregulation of DNA-PKcs and Rad51 has been reported to increase cellular radiosensitivity [11-14]. In contrast, overexpression of Rad51 and Rad52 confers resistance to ionizing radiation [15, 16].

The phosphorylation of the histone protein H2AX (γH2AX) has been used as a measure of the formation and rejoining of DSB induced by different types of chemicals and radiations [17, 18]. H2AX is a histone variant of the H2A family, which is phosphorylated at serine 139 within its conserved COOH-terminal region in response to the presence of DSBs. The early induction of γH2AX by radiation is reported to be mediated mainly by ATM kinase and occurs at the sites of DSBs in the nuclear DNA [19]. The number of γH2AX foci formed in this way has been shown to be directly proportional to the number of DSBs and their dephosphorylation has been correlated with repair of DSBs [20, 21]. The local formation of γH2AX allows microscopic detection of distinct foci that most likely represent a single DSB [20]. The potential to detect a single focus within the nucleus makes this the most sensitive method available for detecting DSBs [22].

Although conventional radiotherapy can directly damage DNA and other organic molecules within cells, most of the damage and the cytotoxicity of such ionizing radiation, comes from the production of ions and free radicals produced via interactions with water. This ‘indirect effect’, a form of oxidative stress, can be modulated by a variety of systems within cells that, in normal situations, maintain homeostasis and redox balance. If cancer cells express high levels of antioxidant redox proteins, they may be more resistant to radiation and so targeting such systems may be a profitable strategy to increase therapeutic efficacy of conventional radiotherapy [23].

In a previous work we developed a melanoma model with different degree of malignancy. Two stable clones A375-A7 and A375-G10 were generated by overexpression of human catalase in amelanotic melanoma A375 cells. Transfected cells with empty vector pcDNA3, A375-PCDNA3, were used as negative control (this control and A375 non-transfected cells showed similar phenotype and comparable performance along experiments). These clones triggered quite distinct phenotypes. Clone A375-G10 raised reactive oxygen species (ROS) levels, which resulted in migration and metastasis by increasing cofilin-1 and CAP1 and decreasing TIAM1 or MTSS1 expression. These proteins are involved in actin polymerization, regulation of cell shape and invasiveness [24-27]. Meanwhile A375-A7 cells reversed the amelanotic phenotype by increasing melanin content and melanocytic differentiation markers. These clones allowed the study of potential differentiation and migration markers and its association with ROS levels *in vitro* and *in vivo*. Herein, we used this melanoma model in order to evaluate the association between radioresistance of melanoma cells and malignancy.

2. MATERIALS AND METHODS

2.1 Cell Culture

Human amelanotic melanoma cell line A375 was kindly donated by Dr. E. Medrano (Huffington Center on Aging, Departments of Molecular & Cellular Biology and Dermatology, Baylor College of Medicine, Houston, Texas, USA). All the experiments with these cells were performed with less than 5 passages from thawing. Two stable clones A375-A7 (melanotic and non-invasive) and A375-G10 (amelanotic and invasive) were originally obtained by transfection of A375 cells with pcDNA3 vector harboring the human catalase cDNA (p-CAT) and selected by geneticin (Sigma, Buenos Aires, Argentina) and clonal dilution. Transfected cells with empty vector pcDNA3, A375-PCDNA3, were used as negative control. Cells were cultured as previously described [28] with the addition of 700 μg/ml geneticin. Cells were regularly tested to be mycoplasma-free.

2.2. Irradiation Experiments and Survival Curves

A ^{137}Cs source (IBL-437C Irradiator, CIS BioInternational) (CEBIRSA, Argentina) was used for gamma irradiations. For clonogenic assays, cells from mid-log growing cultures were plated and incubated for 18 h before irradiation. Control cells were sham irradiated. After irradiation, cells were incubated for 15 days at 37ºC and 5% CO_2. Colonies were fixed and stained. The fraction of clonogenic cells was determined by scoring colonies containing at least 50 cells. Three independent experiments were performed in triplicates for each condition. Survival curves were fitted to the linear–quadratic model (Eq. 1):

$$S = \exp-(\alpha D+\beta D^2) \quad (1)$$

2.3. Bioinformatic Analysis

Differential gene expression among A375-A7, A375-G10 and control A375-PCDNA3 cells was evaluated by the bioinformatic analysis of whole genome microarrays (GeneChip® Human Gene 1.0 ST Array, Affymetrix). The analysis was performed by using the R programming language (2.12.0) [29] and different tools of Bioconductor [30]. The libraries

“affy”, “limma”, “oligo”, “affxparser”, “Iranges”, “gplots”, “Biobase”, “Biostrings”, “cluster”, “annotate”, “org.Hs.eg.db”, “KEGG.db”, “hugene10stprobeset.db”, “Go.db”, “preprocessCore”, “hugene10sttranscriptcluster.db”, “pd.hugene.1.0.st.v1” and “pd.hugene.1.1.st.v1” were used. Background correction and normalization of data were performed by Robust Multi-array Average (rma) both for probeset and core. Differential gene expression was evaluated by Limma (Linear Models for Microarray Data, parameters: lfc=1 or lfc=2 and $p<0.001$). Significant and concordant differences between phenotypes were evaluated by GSEA (Gene Set Enrichment Analysis) [31, 32] with *a priori* defined gene sets collected from KEGG (Kyoto Encyclopedia of Genes and Genomes) [33, 34]. These selected gene sets are associated with cell proliferation and cell death, in particular, MAPK signaling pathways (containing 257 genes), cell cycle (containing 124 genes), apoptosis (containing 86 genes) and p53 signaling pathway (containing 68 genes). An additional gene set related to the antioxidant system was manually defined containing 111 genes to be studied in the same way. Gene networks obtained by the analysis were visualized by GeneMANIA database [35].

2.4. Immunocytofluorescence and quantification of γH2AX

Detection and quantification of γH2AX foci in cells exposed to 2 Gy of gamma radiation or sham-irradiated were performed as previously described [36]. Briefly, 30 minutes after irradiation cells were fixed, permeabilized, blocked, and incubated overnight with a monoclonal anti-γH2AX antibody (Upstate, Lake Placid, NY), which was detected with a fluorescein isothiocyanate-labeled secondary antibody (Sigma, St. Louis, MO). Cells were counterstained and mounted with 4’,6-diamidino-2-phenylindoledihydrochloridedihydrate (DAPI). Two independent experiments were performed in duplicate for each condition.

2.5. Statistical analysis

The results are presented as mean ± SD. Significant changes were assessed using one-way analysis of variance and nonparametric Kruskal-Wallis test followed by Tukey´s or Dunn´s multiple comparison tests to determine significant differences between group means. P values of less than 0.05 were considered significant for all tests.

3. RESULTS AND DISCUSSION

Survival curves were obtained to characterize the radiation response of the clones with different phenotype and control cells (Fig. 1). A375-G10 cells, which exhibit an invasive and metastatic phenotype, were significantly more radioresistant ($p<0.01$) than both A375-A7 and control cells.

Bioinformatic analysis showed a significant decrease of ATM, TP53BP1 and MRE11A expression in A375-G10 cells compared with A375-A7 and controls (Fig. 2). ATM protein, containing a phosphatidyl-inositol 3-kinase like enzyme, is involved in cell cycle control, mitotic recombination, telomere length monitoring and DNA damage response. A rapid increase in kinase activity occurs after exposure to ionizing radiation or in the presence of DSBs [37]. ATM and p53 play a major role in maintaining the integrity of the genome. They both cooperate in enforcing G1 and G2 checkpoint control and ATM-dependent phosphorylation is directly responsible for p53 activation [38]. Alterations in these proteins

may contribute to an increased incidence of genomic changes, such as deletions, translocations and amplifications, which are common during oncogenesis [37].

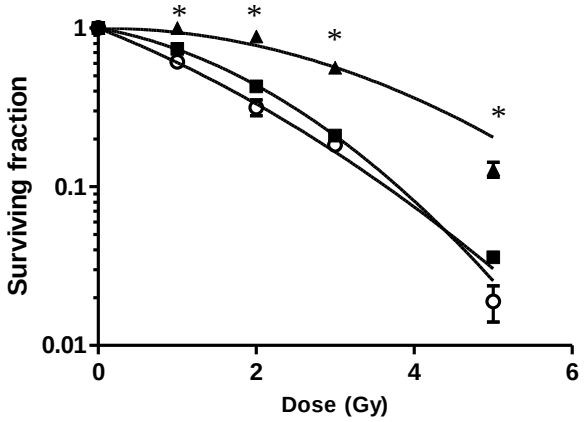

	A375-PCDNA3 (○)	A375-A7 (■)	A375-G10 (▲)
SF2	0.32 ± 0.03	0.43 ± 0.16	0.89 ± 0.05
α (Gy^{-1})	0.45 ± 0.05	0.20 ± 0.05	0
β (Gy^{-2})	0.05 ± 0.02	0.11 ± 0.03	0.06 ± 0.02

Figure 1. Survival curves of melanoma cells after irradiation with gamma rays. Data represent mean ± SD of a representative experiment out of three. Fitted curves are shown. The table shows SF2 and α and β parameters. * p<0.01.

TP53BP1 (tumor protein p53 binding protein 1, 53BP1) is a protein-coding gene which plays a key role in the response to DNA damage, may have a role in checkpoint signaling during mitosis and enhances TP53-mediated transcriptional activation. 53BP1 protein can directly promote ATM kinase activity on multiple substrates. The magnitude of this effect is proportional to the level of Mre11-Rad50-Nbs1 (MRN) complex in the reaction, consistent with the idea that 53BP1 facilitates productive interactions between MRN and ATM and that these interactions are limiting when MRN concentrations fall below a critical threshold [39]. Moreover, siRNA-mediated decrease of 53BP1 levels in human cells reduced the phosphorylation of p53, CHK2, BRCA1, and SMC1 by ATM, particularly after damage induced by low doses of ionizing radiation [39-42]. 53BP1 protein is also phosphorylated by ATM after DNA damage and this phosphorylation is required for ATM-dependent signaling, although recruitment of 53BP1 to DNA damage sites is independent of its phosphorylation [39, 43]. MRE11A gene encodes a nuclear protein involved in homologous recombination, telomere length maintenance, and DNA-DBS repair. This protein is a component of the MRN complex which possesses single-strand endonuclease activity and double-strand-specific 3'-5' exonuclease activity, both provided by MRE11A. Rad50 may be required to bind DNA ends and hold them in close proximity. The complex may also be required for DNA damage

signaling via activation of the ATM kinase. Supporting the importance of the interactions among MRN complex proteins to its stability and function, Mre11 protein mutations that destabilize the MRN complex result in significantly decreased levels of Rad50 and Nbs1 *in vivo*, and knockdown of individual components of MRN can produce decreases in the other two members [44]. Moreover, mutations in human MRE11 lead to ataxia telangiectasia-like disorder [44], in which patients display ataxia and neurodegeneration, resembling the phenotypes of ATM deficiency [45]. Consistent with the involvement of MRN in cell cycle checkpoint signaling, cells from patients with ataxia telangiectasia-like disorder are defective for checkpoint activation [44]. In addition, ataxia telangiectasia-like disorder can display increased tumorigenesis in a p53 null background [44].

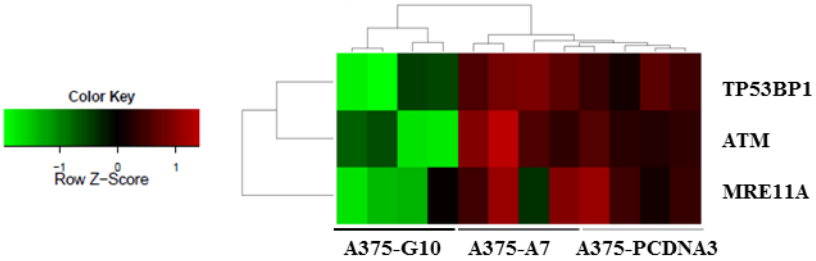

Figure 2. Differential expression profile of genes related to DNA damage response.

Thus, the decrease observed in the levels of TP53BP1 and MRE11A in A375-G10 cells may be related to a defective DNA damage response favored by a reduction of ATM kinase activity, which also exhibited a significant decreased expression. Besides, the low levels of TP53BP1 and MRE11A in A375-G10 cells would help to bypass cell cycle checkpoints. Therefore, the inability of blocking cell cycle progression after DNA damage would turn A375-G10 cells more radioresistant, contributing also to increase genomic instability and malignancy in these cells. Consistent with these results, the GSEA analysis showed in A375-G10 cells, down-regulation of co-expressed genes in the different signaling pathways studied, such as apoptosis, cell cycle and MAPK and p53 signaling pathways. These down-regulated gene sets were, particularly, involved in DNA repair, cell cycle checkpoint, negative regulation of cell cycle and apoptosis (Fig. 3).

Although both A375-A7 and A375-G10 clones overexpressed the antioxidant enzyme catalase, only A375-G10 cells exhibit radioresistance. Both clones showed a different gene expression profile of the antioxidant gene network which could explain, in part, some of the distinctive features of each clone. A375-A7 vs. control cells up-regulated a gene set associated with peroxide and glutathione metabolism while A375-G10 vs. control cells up-regulated a gene set associated with superoxide metabolism and down-regulated the gene set up-regulated in A375-A7 cells. In this sense, the manganese superoxide dismutase was involved as mediator of the adaptive radioresistance to low-dose ionizing radiation [46]. Moreover, radioresistance and shortened G2/M duration were described in cells overexpressing manganese superoxide dismutase [47].

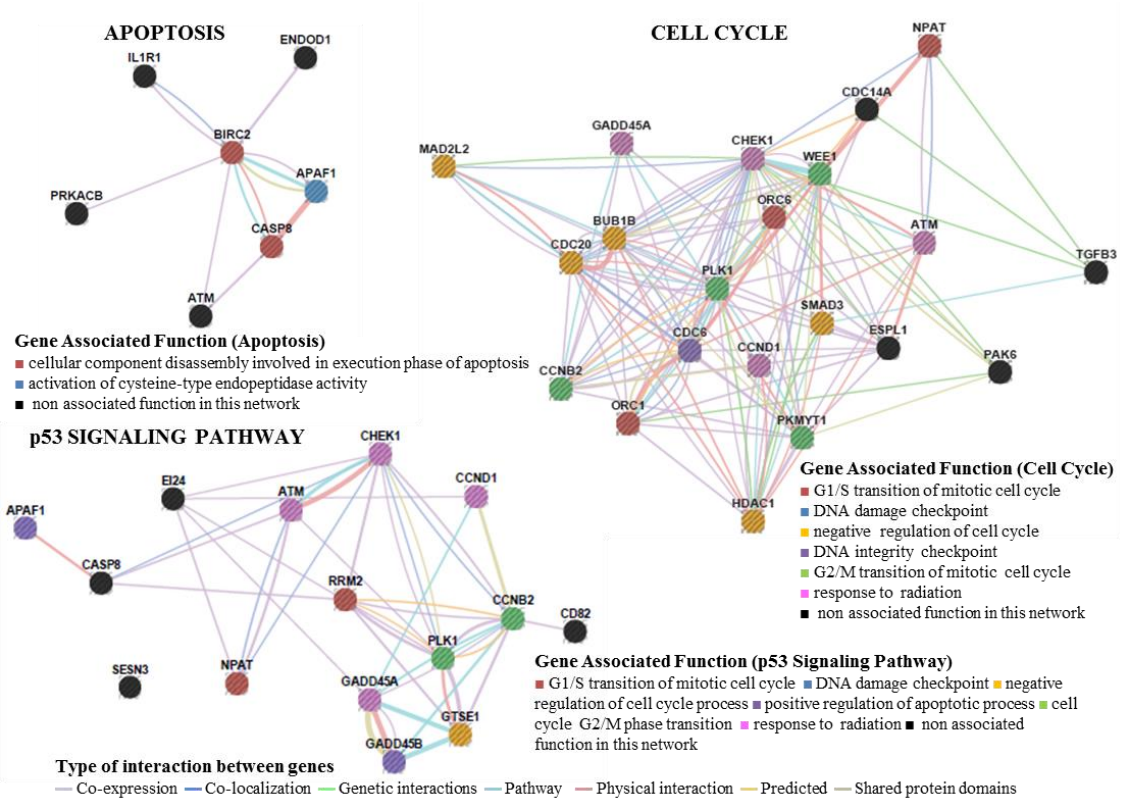

Process or Pathway	Gene	Associated Function
Cell Cycle	ATM	
	CCND1	
	CHEK1	
	PLK1	
	PKMYT1	
	CDC6	
p53 Signaling Pathway	ATM	
	CCND1	
	CHEK1	
	PLK1	
	GTSE1	
	GADD45A	

Figure 3. Gene networks of down-regulated co-expressed genes in A375-G10 cells vs. A375-A7 and control cells. Genes are represented as circles and the links between genes represent the type of interaction among them. The color of each gene represents the associated function in the network. Results of GSEA analysis visualized through GeneMania. Table shows genes with more than one associated function.

Regarding the DSB induction in this melanoma model, A375-A7 and control cells increased the average number of γH2AX foci per nucleus at 30 min after 2 Gy irradiation, while A375-G10 cells did not change the average number of foci post-irradiation (Fig. 4). The lack of γH2AX foci induction in A375-G10 cells is consistent with the gene expression profile of these cells.

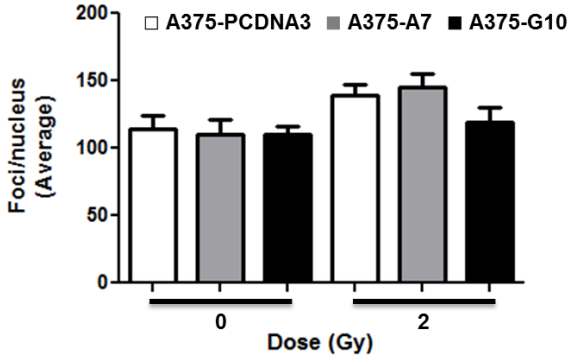

Figure 4. Quantification of nuclear γH2AX foci. Average number of γH2AX foci per nucleus vs. dose. Data represent mean ± SEM of a representative experiment.

4. CONCLUSIONS

We showed in a model of human melanoma cells with different degrees of malignancy a gene expression profile that can be associated with radioresistance and malignant progression. The decreased expression of ATM, TP53BP1 and MRE11A associated with the down-regulation of gene sets involved in DNA repair, cell cycle checkpoint, negative regulation of cell cycle and apoptosis could favor the radioresistance and the low sensing of DNA-damage observed in A375-G10 clone which exhibits the more aggressive phenotype, being invasive and metastatic.

5. REFERENCES

1. Garbe, C., et al., Diagnosis and treatment of melanoma: European consensus-based interdisciplinary guideline. *Eur J Cancer*, **46**, pp. 270-283 (2010).
2. Mandala, M. and Massi, D., Tissue prognostic biomarkers in primary cutaneous melanoma. *Virchows Arch*, **464**, pp. 265-281 (2014).
3. Jemal, A., et al., Cancer statistics, 2006. *CA Cancer J Clin*, **56**, pp. 106-130 (2006).
4. Batus, M., et al., Optimal management of metastatic melanoma: current strategies and future directions. *Am J Clin Dermatol*, **14**, pp. 179-194 (2013).
5. Leu, J.D., et al., Enhanced cellular radiosensitivity induced by cofilin-1 over-expression is associated with reduced DNA repair capacity. *Int J Radiat Biol*, **89**, pp. 433-444 (2013).
6. Harrington, K., et al., Molecular biology for the radiation oncologist: the 5Rs of radiobiology meet the hallmarks of cancer. *Clin Oncol (R Coll Radiol)*, **19**, pp. 561-571 (2007).
7. van Gent, D.C., et al., Chromosomal stability and the DNA double-stranded break connection. *Nat Rev Genet*, **2**, pp. 196-206 (2001).
8. Rattay, T. and Talbot, C.J., Finding the genetic determinants of adverse reactions to radiotherapy. *Clin Oncol (R Coll Radiol)*, **26**, pp. 301-308 (2014).
9. Moynahan, M.E. and Jasin, M., Mitotic homologous recombination maintains genomic stability and suppresses tumorigenesis. *Nat Rev Mol Cell Biol*, **11**, pp. 196-207 (2010).

10. Valerie, K. and Povirk, L.F., Regulation and mechanisms of mammalian double-strand break repair. *Oncogene*, **22**, pp. 5792-5812 (2003).
11. Gu, Y., et al., Ku70-deficient embryonic stem cells have increased ionizing radiosensitivity, defective DNA end-binding activity, and inability to support V(D)J recombination. *Proc Natl Acad Sci U S A*, **94**, pp. 8076-8081 (1997).
12. Taki, T., et al., Antisense inhibition of the RAD51 enhances radiosensitivity. *Biochem Biophys Res Commun*, **223**, pp. 434-438 (1996).
13. Harima, Y., et al., Expression of Ku80 in cervical cancer correlates with response to radiotherapy and survival. *Am J Clin Oncol*, **26**, pp. e80-e85 (2003).
14. Bracalente, C., et al., Induction and persistence of large gammaH2AX foci by high linear energy transfer radiation in DNA-dependent protein kinase-deficient cells. *Int J Radiat Oncol Biol Phys*, **87**, pp. 785-794 (2013).
15. Vispe, S., et al., Overexpression of Rad51 protein stimulates homologous recombination and increases resistance of mammalian cells to ionizing radiation. *Nucleic Acids Res*, **26**, pp. 2859-2864 (1998).
16. Park, M.S., Expression of human RAD52 confers resistance to ionizing radiation in mammalian cells. *J Biol Chem*, **270**, pp. 15467-15470 (1995).
17. Rogakou, E.P., et al., Megabase chromatin domains involved in DNA double-strand breaks in vivo. *J Cell Biol*, **146**, pp. 905-916 (1999).
18. Tanaka, T., et al., Cytometry of ATM activation and histone H2AX phosphorylation to estimate extent of DNA damage induced by exogenous agents. *Cytometry A*, **71**, pp. 648-661 (2007).
19. Burma, S., et al., ATM phosphorylates histone H2AX in response to DNA double-strand breaks. *J Biol Chem*, **276**, pp. 42462-42467 (2001).
20. Rothkamm, K. and Lobrich, M., Evidence for a lack of DNA double-strand break repair in human cells exposed to very low x-ray doses. *Proc Natl Acad Sci U S A*, **100**, pp. 5057-5062 (2003).
21. Kinner, A., et al., Gamma-H2AX in recognition and signaling of DNA double-strand breaks in the context of chromatin. *Nucleic Acids Res*, **36**, pp. 5678-5694 (2008).
22. Ismail, I.H., et al., An optimized method for detecting gamma-H2AX in blood cells reveals a significant interindividual variation in the gamma-H2AX response among humans. *Nucleic Acids Res*, **35**, pp. e36 (2007).
23. Zhang, Y. and Martin, S.G. Redox proteins and radiotherapy. *Clin Oncol (R Coll Radiol)*, **26**, pp. 289-300 (2014).
24. Sidani, M., et al., Cofilin determines the migration behavior and turning frequency of metastatic cancer cells. *J Cell Biol*, **179**, pp. 777-791 (2007).
25. Moriyama, K. and Yahara, I., Human CAP1 is a key factor in the recycling of cofilin and actin for rapid actin turnover. *J Cell Sci*, **115**, pp. 1591-1601 (2002).
26. Liu, K., et al., Downregulation of metastasis suppressor 1(MTSS1) is associated with nodal metastasis and poor outcome in Chinese patients with gastric cancer. *BMC Cancer*, **10**, pp. 428 (2010).
27. Uhlenbrock, K., et al., The RacGEF Tiam1 inhibits migration and invasion of metastatic melanoma via a novel adhesive mechanism. *J Cell Sci*, **117**, pp. 4863-4871 (2004).
28. Ibanez, I.L., et al., Phosphorylation and subcellular localization of p27Kip1 regulated by hydrogen peroxide modulation in cancer cells. *PLoS One*, **7**, pp. e44502 (2012).
29. Team, R.D.C., *R: A language and environment for statistical computing*. R Foundation for Statistical Computing: Vienna, Austria. (2006)
30. Gentleman, R.C., et al., Bioconductor: open software development for computational biology and bioinformatics. *Genome Biol*, **5**, pp. R80 (2004).

31. Subramanian, A., et al., Gene set enrichment analysis: a knowledge-based approach for interpreting genome-wide expression profiles. *Proc Natl Acad Sci U S A*, **102**, pp. 15545-15550 (2005).
32. Mootha, V.K., et al., PGC-1alpha-responsive genes involved in oxidative phosphorylation are coordinately downregulated in human diabetes. *Nat Genet*, **34**, pp. 267-273 (2003).
33. Kanehisa, M. and Goto, S., KEGG: kyoto encyclopedia of genes and genomes. *Nucleic Acids Res*, **28**, pp. 27-30 (2000).
34. Kanehisa, M., et al., KEGG for integration and interpretation of large-scale molecular data sets. *Nucleic Acids Res*, **40**, pp. D109-D114 (2012).
35. Warde-Farley, D., et al., The GeneMANIA prediction server: biological network integration for gene prioritization and predicting gene function. *Nucleic Acids Res*, **38**, pp. W214-W220 (2010).
36. Ibanez, I.L., et al., Induction and rejoining of DNA double strand breaks assessed by H2AX phosphorylation in melanoma cells irradiated with proton and lithium beams. *Int J Radiat Oncol Biol Phys*, **74**, pp. 1226-1235 (2009).
37. Mavrou, A., et al., The ATM gene and ataxia telangiectasia. *Anticancer Res*, **28**, pp. 401-405 (2008).
38. McKinnon, P.J., ATM and ataxia telangiectasia. *EMBO Rep*, **5**, pp. 772-776 (2004).
39. Lee, J.H., et al., 53BP1 promotes ATM activity through direct interactions with the MRN complex. *EMBO J*, **29**, pp. 574-585 (2010).
40. DiTullio, R.A., Jr., et al., 53BP1 functions in an ATM-dependent checkpoint pathway that is constitutively activated in human cancer. *Nat Cell Biol*, **4**, pp. 998-1002 (2002).
41. Jowsey, P.A., et al., Human PTIP facilitates ATM-mediated activation of p53 and promotes cellular resistance to ionizing radiation. *J Biol Chem*, **279**, pp. 55562-55569 (2004).
42. Wang, B., et al., 53BP1, a mediator of the DNA damage checkpoint. *Science*, **298**, pp. 1435-1438 (2002).
43. Zgheib, O., et al., ATM signaling and 53BP1. *Radiother Oncol*, **76**, pp. 119-122 (2005).
44. Lamarche, B.J., et al., The MRN complex in double-strand break repair and telomere maintenance. *FEBS Lett*, **584**, pp. 3682-3695 (2010).
45. Taylor, A.M., et al., Ataxia-telangiectasia-like disorder (ATLD)-its clinical presentation and molecular basis. *DNA Repair (Amst)*, **3**, pp. 1219-1225 (2004).
46. Fan, M., et al., Nuclear factor-kappaB and manganese superoxide dismutase mediate adaptive radioresistance in low-dose irradiated mouse skin epithelial cells. *Cancer Res*, **67**, pp. 3220-3238 (2007).
47. Takada, Y., et al., Role of reactive oxygen species in cells overexpressing manganese superoxide dismutase: mechanism for induction of radioresistance. *Mol Cancer Res*, **1**, pp. 137-146 (2002).